Chapter 4 : Effects of spherical hybrid silica-molybdenum disulphide on the lubrication

This investigation examines the performance of a hybrid structure composed of spherical silica and lamellar MoS_2, engineered into a composite sphere, as an antiwear and antifriction additive in vegetable oil for steel-on-steel tribological pairs. A four-ball tribo-tester was employed under fully flooded conditions to assess antiwear and extreme pressure properties. Post-testing, the oil and wear debris were analysed to understand the lubrication mechanism. Additionally, X-ray Photoelectron Spectroscopy was used to identify changes in the speciation of the tribofilm formed during the tests.

4.1. Characterization of nanoparticles

4.1.1. X-ray diffraction results of particles

Figure 4.1 presents the XRD patterns for MoS_2, SiO_2, and their hybrid microspheres, measured over a 2θ range of 10° to 80° with a step size of 0.02° and a scan rate of 5°/min. The XRD pattern of MoS_2, shown in Figure 4.1a, reveals prominent diffraction peaks at 2θ of 13.98°, 33.24°, 39.86°, and 58.89°, corresponding to the (002), (101), (103), and (110) lattice planes, respectively. In Figure 4.1b, the XRD pattern of amorphous silicon dioxide (SiO_2) displays a broad diffraction peak at 2θ of 23.5°, attributing to the (101) plane [88]. Vertical reference lines are included in both Figures 4.1a and 4.1b to align with the peaks observed in the XRD pattern of hybrid microspheres, illustrating that all characteristic peaks of the individual components are retained in the hybrid material.

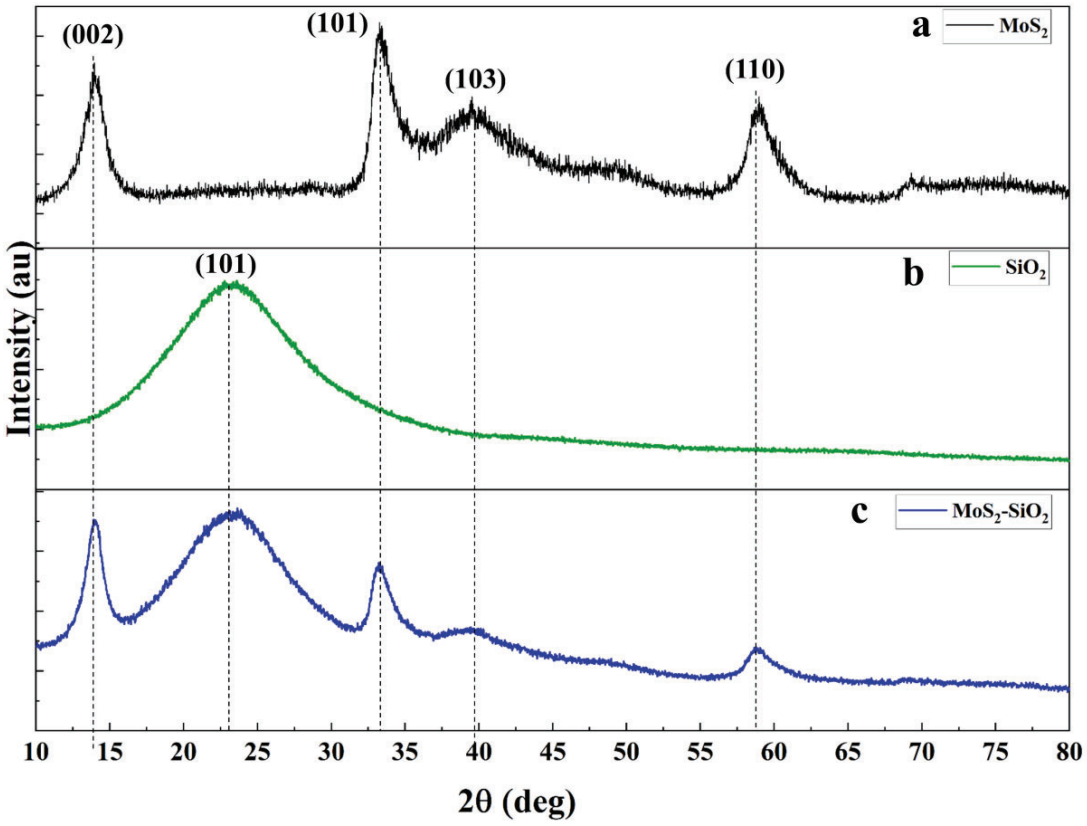

Figure 4.1 XRD patterns of nanomaterials

These analyses indicate that no phase transformation occurs in the final hybrid product, preserving the structural integrity of the individual components. However, the peaks associated with MoS_2, is broadened, likely due to alterations in the atomic arrangement within the material [89]. The changes in peak intensity can be attributed to the compositional modifications during hybrid formation. Notably, the intensity difference between the (002) and (101) planes in the XRD pattern of the hybrid shows a subtle variation compared to pure MoS_2.

A closer examination revealed that the growth of silica on the MoS_2 surface induces strain within the material, evidenced by an increase in the full width at half maxima (FWHM) of the (002) peak from 1.1021° to 1.5744°. This increase suggests a relative positional shift

of atoms within the crystal lattice. The strain weakens the lamellar structure of MoS_2 by expanding the interlayer spacing, which promotes sheet exfoliation. This exfoliation effect in the hybrid material could explain the observed enhancement in the intensity of the (002) plane. The broader peaks and increased FWHM collectively highlight the structural modifications and interactions between silica and MoS_2, which play a critical role in the hybrid's properties and functionality.

The formation of spherical hybrids is influenced by the relative concentration of MoS_2 to silica and the amount of ammonia used during the reaction. Higher ammonia concentrations lead to larger silica spheres, while lower concentrations result in smaller spheres [90]. In this study, MoS_2 was dispersed in a mixture of ethanol and water, followed by the deposition of silica onto the MoS_2 surface. This process caused the MoS_2 sheets to bend, forming spherical structures, a phenomenon also observed by Kwok et al. [91]. The bending of MoS_2 sheets alters the relative positions of atoms within the stacked lamellae, which is reflected in the broadening of XRD peaks. The curvature of the MoS_2 sheets creates uneven interplanar distances, weakening van der Waals interactions between the layers and enabling the sheets to shear more easily.

4.1.2. Morphological characterization of particles

The field emission scanning electron micrograph of MoS_2 is shown in Figure 4.2. Figure 4.3. The SEM images of the hybrid reveal spherical clusters of SiO_2-MoS_2 ranging a size of 400 to 600 nm, with an average particle size of 500 nm. These spherical structures exhibit a corona-like arrangement where silica encapsulates and interweaves with the MoS_2 sheets (Figure 4.4). This architecture is confirmed through the EDS spectra, which indicate the presence of Si, O, Mo, and S, verifying the elemental composition of the SiO_2-MoS_2 hybrid. To provide a quantitative understanding of the particle size

distribution, Figure 4.5 (c) illustrates a statistical analysis of particle sizes measured at numerous locations on the sample. The data, when fitted to a normal distribution, validate the uniformity in particle formation. This uniformity is crucial for ensuring consistency in material properties across the batch, such as density, porosity, and mechanical strength. Figure 4.4 illustrates how MoS_2 sheets are embedded and coated with silica, forming a spherical corona. This structure results from the unique gelation and wrapping mechanism during synthesis.

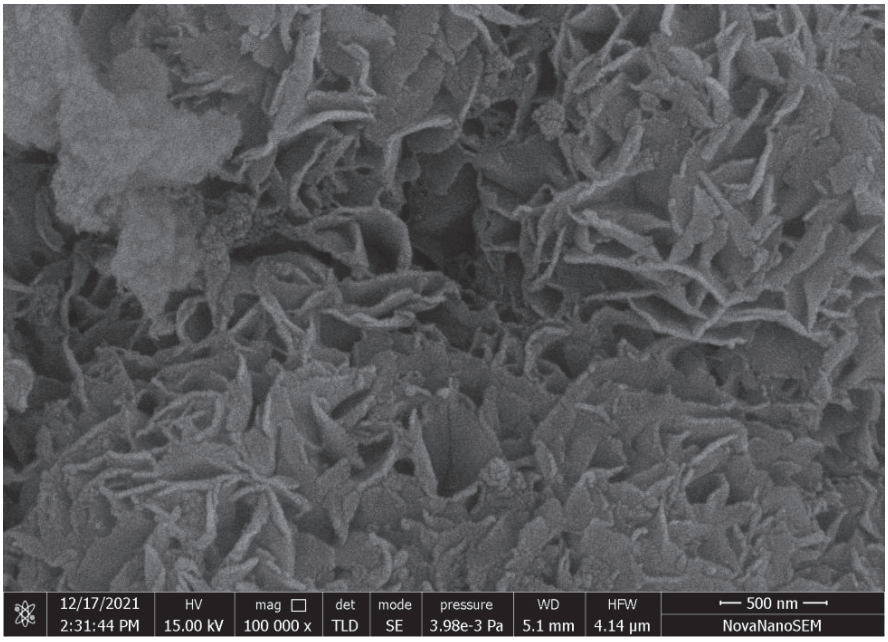

Figure 4.2 SEM image of MoS_2 sheets

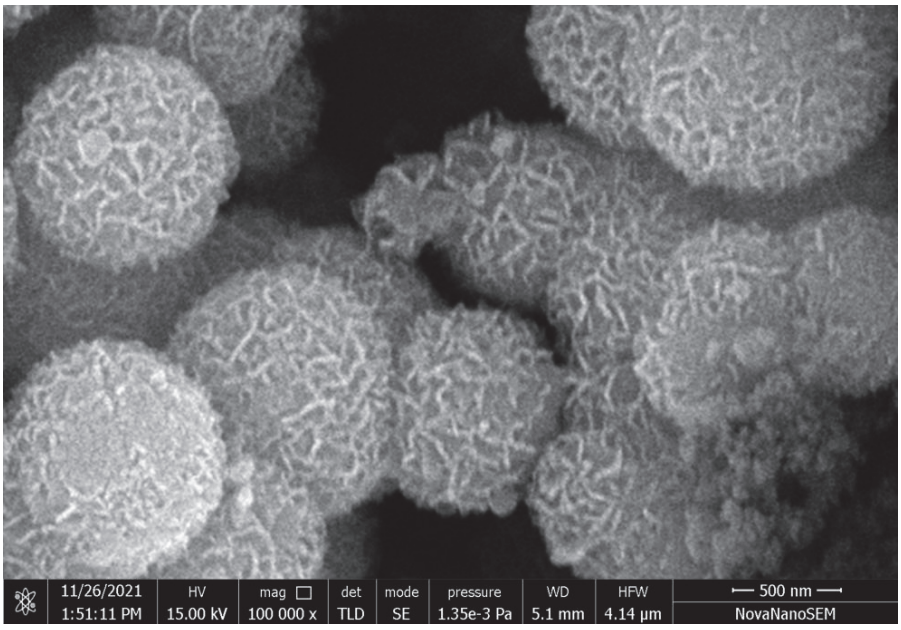

Figure 4.3 SEM images of hybrid SiO_2-MoS_2 particles

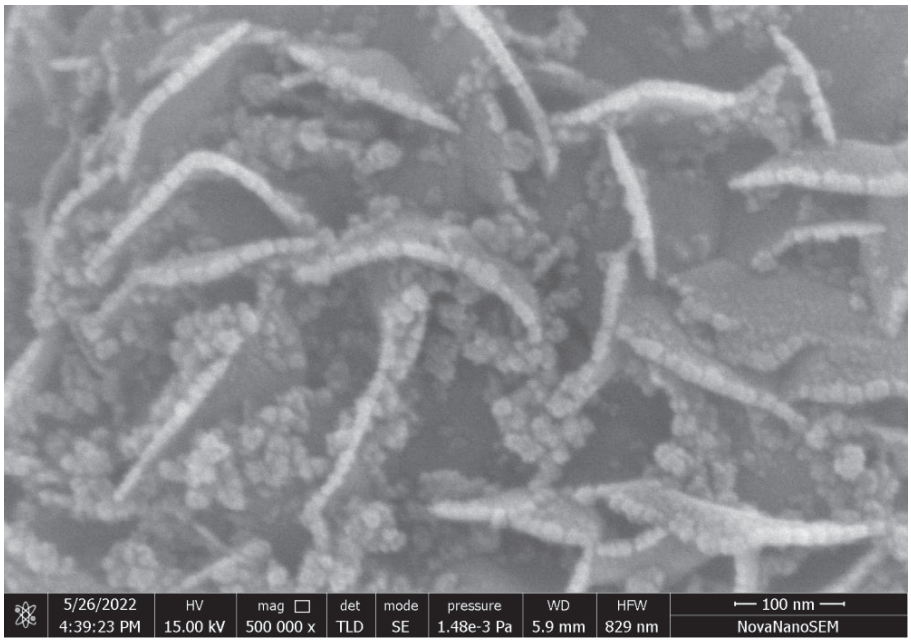

Figure 4.4 Shows the distribution of SiO_2 particles along with the MoS_2 sheets

The high-resolution transmission electron microscopy (HR-TEM) image (Figure 4.6) provides an in-depth visualization of the hybrid microspheres. The MoS_2 nanosheets are arranged in the form hierarchical microspheres and silica particles. Importantly, each

sheet of MoS_2 in the hybrid microsphere contains limited number of molecular lamellae with interlamellar spacing of 0.62 nm.

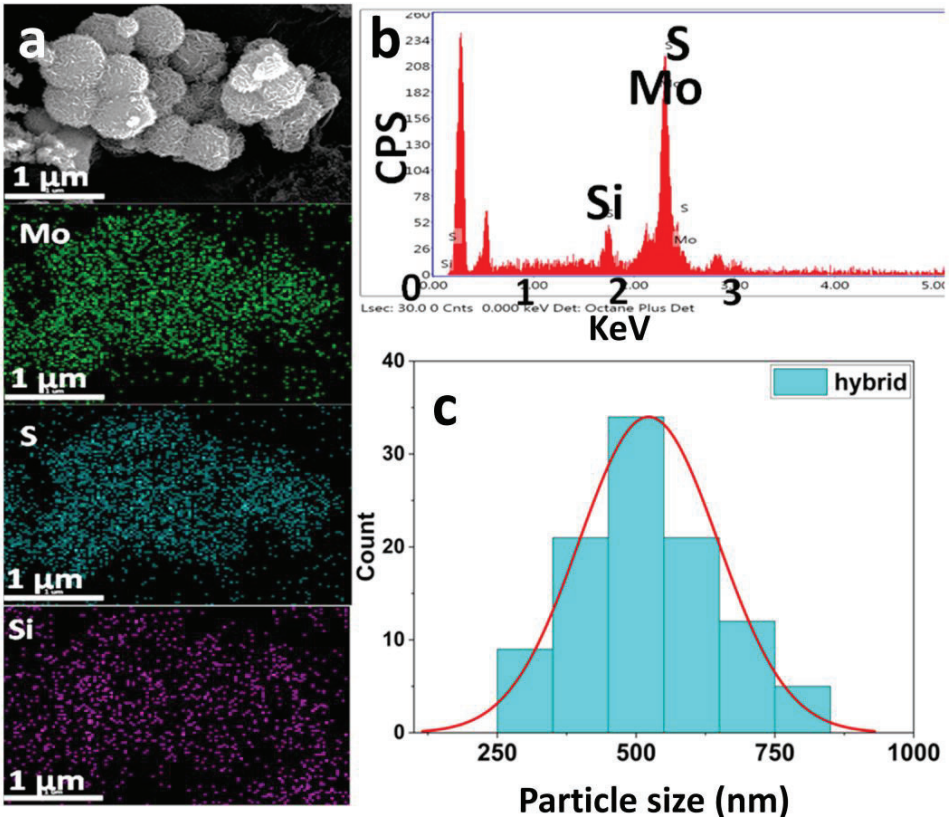

Figure 4.5(a) EDS mapping (b) EDS Spectra (c) size distribution of hybrid particles

Figure 4.6 TEM images of hybrid particles

The unique morphology and structure of the silica-MoS_2 hybrid spheres offer several advantages:

- **Lightweight composition:** The voids within the spheres reduce the overall density, making them suitable for applications requiring lightweight materials.
- **Porosity:** The voids and corona-like arrangement increase the surface area, enhancing catalytic or adsorption capabilities.
- **Structural integrity:** The wrapping of silica around MoS_2 sheets ensures stability while maintaining flexibility, which may be useful in dynamic environments.

4.2. Formulation stability

Among vegetable oils, castor oil stands out for its superior viscosity at room temperature and its excellent film-forming capability, attributed to its strong affinity for metallic surfaces. In this study, the hybrid nanoparticles were incorporated into castor oil at four different weight percentages (0.025, 0.05, 0.075, and 0.1 wt%) to evaluate their dispersion stability. These mixtures were visually monitored over time to assess stability, with digital images captured at intervals.

At the lowest concentration of 0.025 wt%, a slight and transient change in oil colour was observed, suggesting limited dispersion stability initially. However, at higher concentrations (0.05, 0.075, and 0.1 wt%), no such visible colour change was detected. Over time, the nanoparticles in all samples gradually settled, taking approximately 28 days to completely sediment, even without the use of any dispersion agent to enhance stability. Figure 4.7 illustrates the dispersion stability of the hybrid over a 120-hour period across all concentrations. The results indicate that dispersion stability is robust for

all formulations, with the higher nanoparticle concentrations demonstrating the most stable dispersion behaviour throughout the observation period.

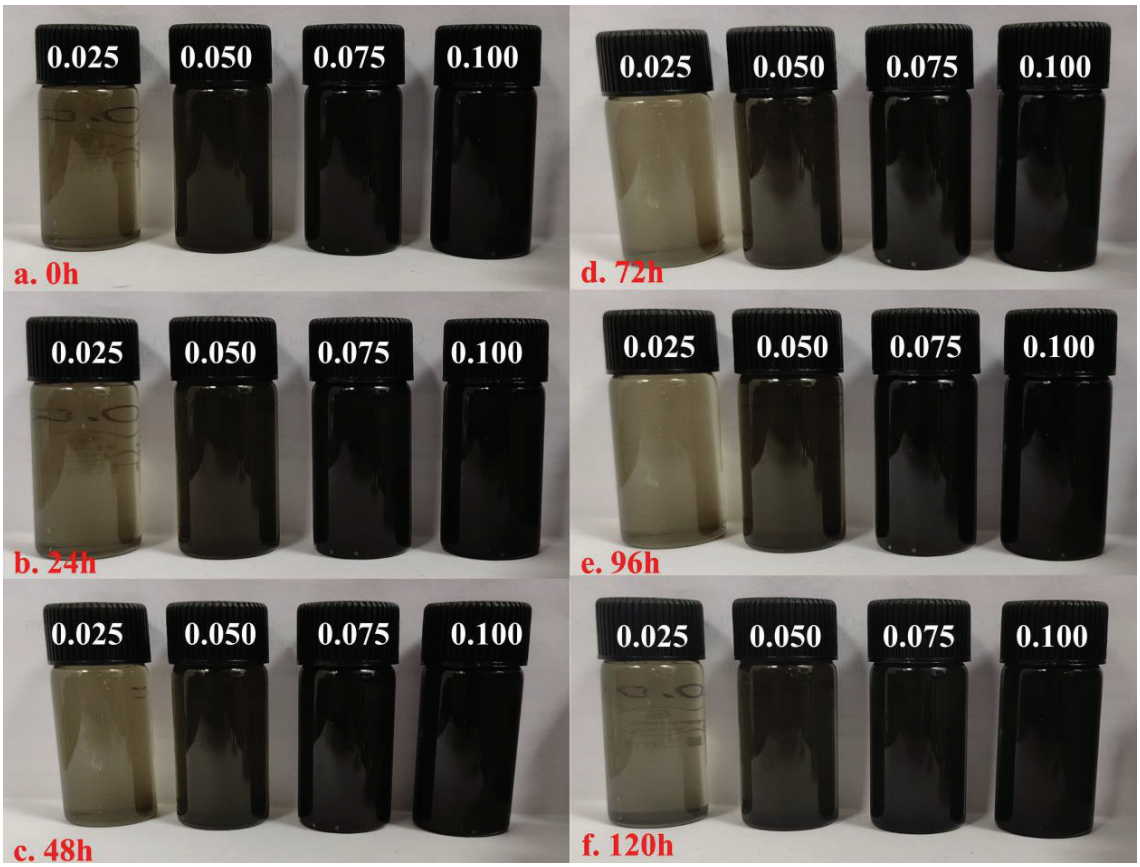

Figure 4.7: Digital images of formulation stability shown for various concentrations of hybrid nanolubricants

The higher concentration of ammonia, combined with rapid drying, results in the formation of larger silica particles. These particles tend to have a lower density due to the evaporation of entrapped solvent during the drying process. Despite their larger size, these low-density silica particles exhibit excellent stability when dispersed in oil. This is because lighter particles experience reduced sedimentation, as sedimentation velocity is directly proportional to particle density. When silica is combined with MoS_2 to form a hybrid structure, the overall density of the hybrid becomes lower than that of pure MoS_2. This reduction in density enhances the hybrid's dispersion stability in oil, as the lighter

particles are less likely to settle over time, ensuring a more uniform and stable suspension.

4.3. Tribological evaluation

Friction is an inevitable phenomenon at contacting surfaces, leading to energy loss [92]. Figures 4.8 illustrate the average COF as a function of nanoparticle concentration for various formulations, including a hybrid of molybdenum disulfide (MoS_2) and silica (SiO_2), individual MoS_2, and SiO_2, along with pure base oil for comparison. These results, based on three repeated tests, highlight the influence of nanoparticle additives on lubrication performance. Figure 4.8(a) specifically depicts the COF variation over time for pure oil and a lubricant containing 0.05 wt% nanoparticles. The time-dependent behaviour provides insight into the role of nanoparticles during the initial running-in period and subsequent steady-state lubrication. At the beginning of the tests, all lubricant formulations, including pure oil, exhibit higher COF values due to the running-in period. During this phase, surface asperities interact and undergo wear-in adjustments under lubrication. The introduction of nanoparticles significantly alters this process by modifying the interaction dynamics at the tribological interface. SiO_2 nanoparticles, known for their hardness and chemical stability, act as third-body abrasives during the running-in phase. These particles fill surface asperities, contributing to a smoothing effect through mild abrasion. This surface refinement reduces roughness more rapidly, enabling the COF to stabilize sooner compared to pure oil.

MoS_2 nanoparticles, characterized by their lamellar structure and low shear strength, enhance lubrication by reducing friction between asperities. However, MoS_2 stabilizes more slowly than SiO_2 during the running-in period. This slower stabilization is attributed to the presence of unexfoliated MoS_2 particles, which cause mild abrasion at the

tribological interface before forming a uniform lubricating film. Over time, these particles exfoliate and align, resulting in a significant reduction in COF and improved steady-state lubrication.

Hybrid nanomaterial, comprising MoS_2 and SiO_2 nanoparticles exhibits a synergistic effect, balancing the advantages of both materials. SiO_2 accelerates the surface smoothing process during the running-in phase, while MoS_2 provides sustained friction reduction in the steady state. This combination results in superior tribological performance compared to individual nanoparticles or pure oil. After the running-in period, the COF stabilizes for all formulations, with nanoparticles-enriched lubricants consistently outperforming pure oil. The steady-state COF is significantly lower for lubricants containing MoS_2, SiO_2, or their hybrid, demonstrating the effectiveness of nanoparticles in maintaining a protective film under prolonged sliding conditions [93].

Figures 4.8b and 4.8c present the variation of COF and wear scar diameter (WSD) with nanoparticles concentration. Compared to pure oil, silica shows minor improvements, while MoS_2 and hybrid nanoparticles-based lubricants demonstrate a reduction in COF up to 0.05 wt% concentration, followed by an increase as the concentration reaches 0.1 wt%. At 0.05 wt%, the average COF values are 0.0323 for the hybrid lubricant, 0.0419 for MoS_2, and 0.0510 for silica, with pure oil having the highest COF of 0.0604.

The reduction in friction and wear is attributed to nanoparticles functioning as effective anti-wear and anti-friction additives. The hybrid particles exhibit the most significant reduction, indicating a synergistic effect between the two types of particles [94–96]. The COF and wear decrease with hybrid nanoparticles up to 0.05 wt% due to optimal lubrication and surface mending. Beyond 0.05 wt%, increased particle concentration leads to direct interaction with the surface, causing abrasion and raising friction and wear.

Figure 4.8e compares the extreme pressure properties of the hybrid lubricant and pure oil. In the initial test at 80 kgf (784 N), the result significantly deviated from the compensation line. Subsequent testing at a lower load of 63 kgf (617.4 N), close to the compensation line, determined the last non-seizure load (LNL), which was identical for both lubricants. Region *ab* represents an impending seizure characterized by heavy plastic deformation. Point *d* indicates the load before welding, recorded at 126 kgf (1234.8 N) for both lubricants, although the hybrid lubricant showed a smaller wear scar. The weld load was 160 kgf (1568 N) for all lubricants, as the particle concentration was insufficient to influence the deformed tribosurface at this stage.

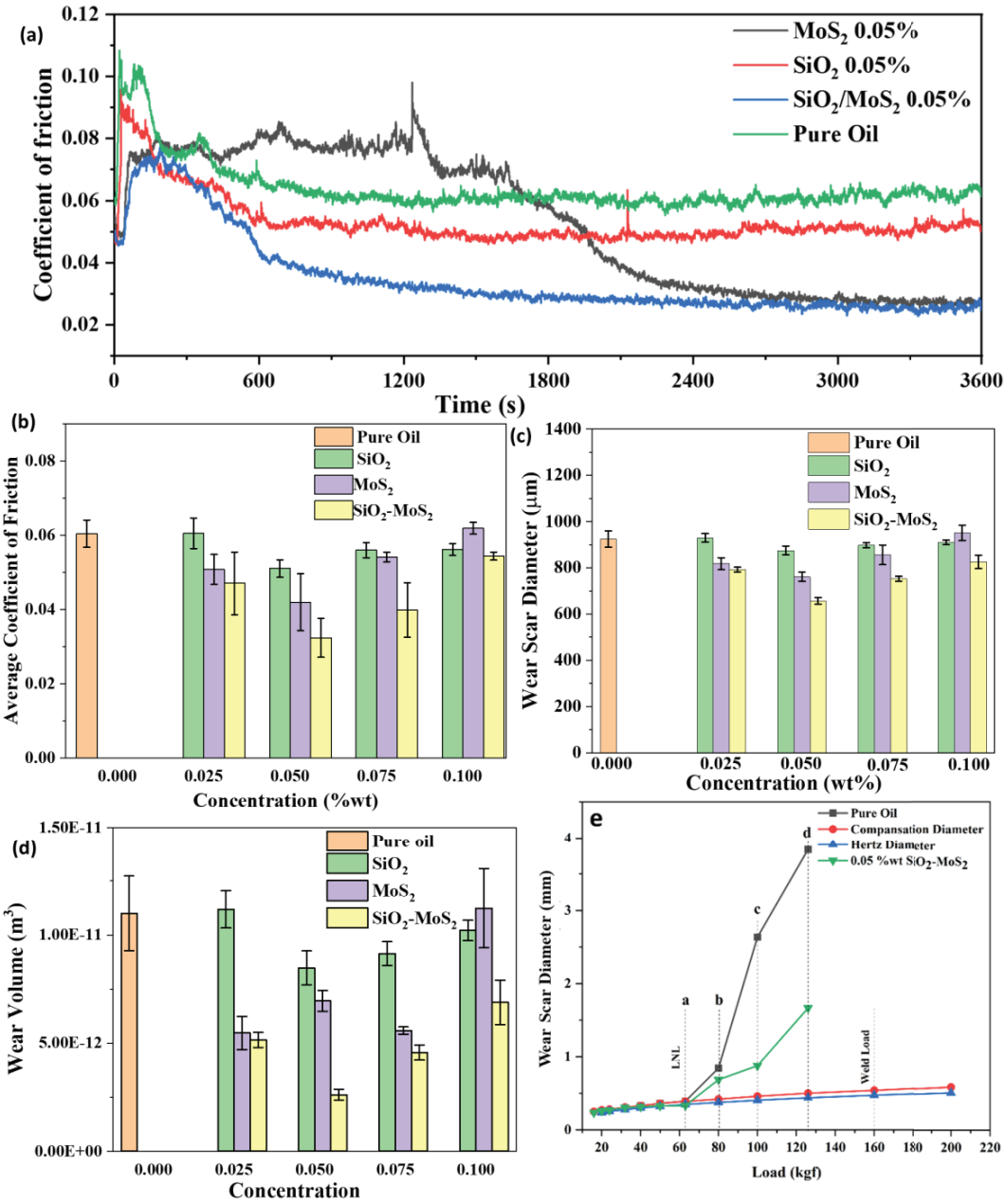

Figure 4.8 Tribological test results (test conditions as per ASTM D-4172): (a) COF versus time, (b) average COF versus concentration, (c) wear scar diameter (WSD) versus concentration, (d) wear volume plotted against concentration of nanoparticles, and (e) wear scar diameter of hybrid-lubricated ball at 0.05 wt% with varying load

4.4. Worn surface analysis

4.4.1. SEM images of worn surface

Figure 4.9 presents SEM images of the wear scars developed on the steel balls during the lubrication tests. These images illustrate the after-lubrication tests with pure oil, single nanoparticle-enhanced lubricant, and hybrid nanoparticle-based nanolubricant. The examination of worn steel ball surfaces under higher magnification reveals distinct features corresponding to different lubrication conditions. The ball lubricated with pure oil displays pronounced wear in the form of deep grooves accompanied by consistent, regular scratches. In contrast, the ball lubricated with silica-mixed oil exhibits scratches caused by abrasive wear, appearing irregular or dashed in nature. Surfaces lubricated with MoS_2-based oil appear smoother; however, closer inspection reveals signs of material displacement, indicating localized deformation. The hybrid sphere-lubricated surface, on the other hand, shows a combination of smooth areas interspersed with irregular scratches.

The wear mechanism varies significantly with the type of lubricant, as indicated by the wear map shown in Figure 4.10. For pure oil, the wear mode is entirely adhesive, characterized by material transfer between contacting surfaces. In the case of silica-lubricated surfaces, abrasive wear dominates, with particles contributing to material removal. For MoS_2-lubricated surfaces, adhesion combined with surface ploughing is the primary wear mechanism, resulting in smoother but deformed regions. When hybrid nanoparticles are used, the wear mechanism involves a mix of abrasive wear and localized chip removal, driven by adhesion. Additionally, elemental mapping of the worn surfaces highlights the formation of a tribo-layer, confirming the presence and

contribution of the lubricant additives. The tribo-layer plays a critical role in protecting the surfaces and reducing wear during tribo-performance.

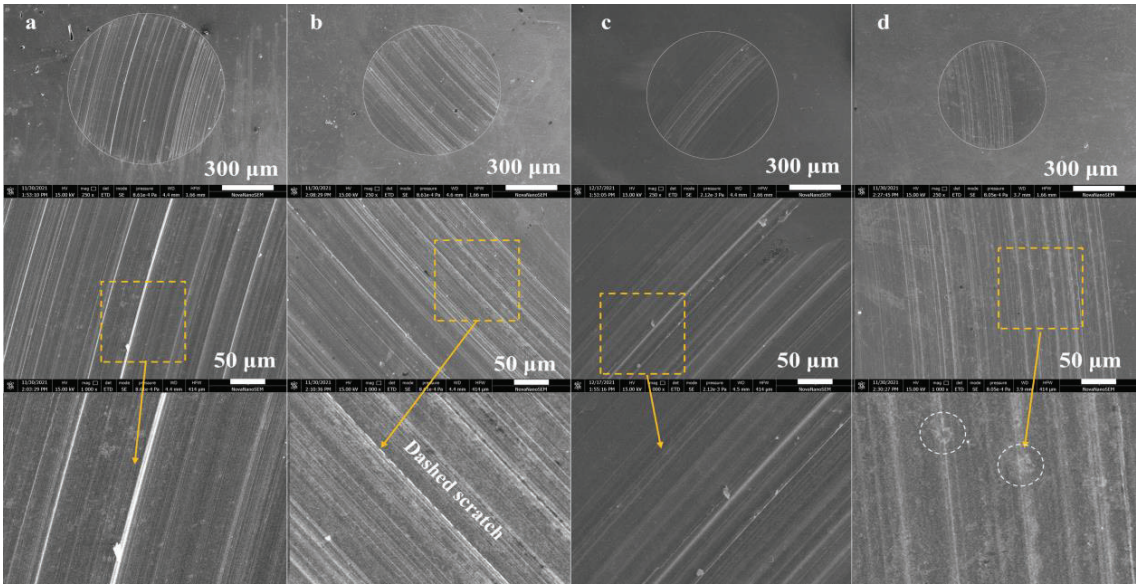

*Figure 4.9: Wear scar developed on the steel balls (test condition as per ASTM D-4172) with corresponding enlarged images for the case of (*a*) pure oil, (*b*) 0.05 wt% SiO_2, (*c*) 0.05 wt% MoS_2, and (*d*) 0.05 wt% SiO_2–MoS_2*

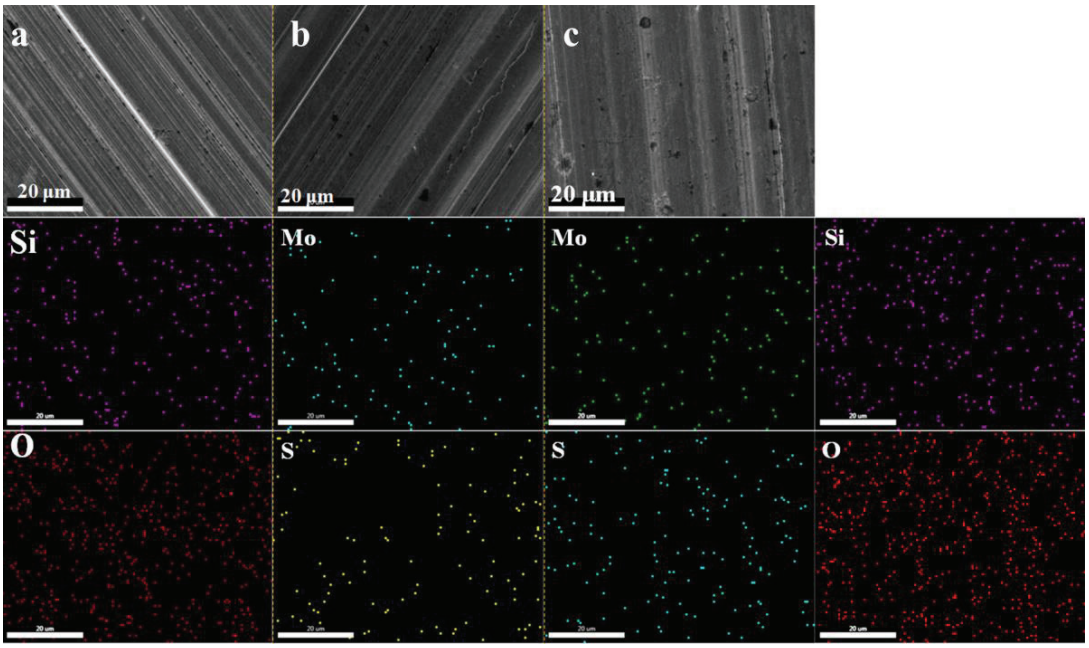

Figure 4.10 EDS-based elemental mapping of worn surfaces of steel balls after lubrication tests with: (a) silica-based lubricant, (b) MoS_2–based lubricant, and (c) hybrid material-based lubricant

4.4.2. Atomic force micrographs (AFM) of different worn surfaces

The surface roughness and its associated parameters play a critical role in determining the tribological performance of a lubricated system.

1. Role of surface roughness in tribology

Surface roughness is an essential aspect of tribological interfaces, affecting friction, wear, and lubrication. The choice of roughness parameters depends on the intended application. For example, in effectively lubricated systems, surfaces with quasi-planar plateaus and narrow grooves provide optimal performance as they facilitate stable lubrication and oil retention.

2. Profile root mean square roughness (Rq)

Definition and sensitivity: Rq represents the root mean square (RMS) value of the surface height variations and is more sensitive to larger deviations in height than the arithmetic mean roughness (Ra). This makes Rq particularly useful in evaluating the surface for applications requiring precise control of contact and lubrication.

Findings: The 0.05 wt% silica lubricated surface exhibited the highest Rq, indicating a surface with significant height variations. Conversely, the hybrid (SiO_2-MoS_2) lubricated surface had the lowest Rq, suggesting a smoother surface with reduced height deviations.

3. Skewness (Rsk)

Negative skewness: All lubricated surfaces showed negative skewness, implying that their surfaces predominantly consist of valleys rather than peaks. This is advantageous because such surfaces retain lubricants more effectively, promoting reduced friction and wear.

Mechanism: The abrasive action of particles (e.g., SiO_2) during sliding causes peaks to break, contributing to the negative skewness. Deep grooves resulting from this abrasion further amplify the negativity of Rsk, as noted by Gadelmawla et al [97].

4. Kurtosis (Rku)

Platykurtic distribution (Rku < 3): The kurtosis values for all surfaces indicated a platykurtic distribution, characterized by a flatter profile with fewer extreme peaks and valleys. Such surfaces are desirable as they reduce the risk of localized stress concentrations and enhance the load-bearing capacity.

Hybrid system behaviour: The hybrid lubricated surface exhibited Rku values indicative of a surface where peaks and valleys are closer to the mean line, aligning well with Gaussian distribution characteristics.

5. Mean spacing of peaks (Sm)

Lowest Sm for hybrid system: The hybrid lubricated system had the lowest mean spacing (Sm) at the mean line, signifying that the asperities are closely packed. This contributes to a smoother contact interface, reducing wear and improving lubrication efficiency.

6. Mean slope of profile (Δ_a)

Flatter asperity profile: Among the systems studied, the hybrid system demonstrated the lowest mean slope of the surface profile. This indicates that the surface asperities are flatter, contributing to reduced friction and enhanced load distribution.

7. Surface comparison and bearing applications

Asperity profile: Figure 4.11 (as referenced) compares worn surfaces lubricated with different systems, including pure castor oil, SiO_2-doped oil, MoS_2-doped oil, and hybrid SiO_2-MoS_2-doped oil. The hybrid system showed the smoothest and flattest asperity profile.

Bearing ratio curve and AFM analysis: Figure 4.12 highlights the bearing ratio curve and corresponding Atomic Force Microscopy (AFM) line roughness profile for the worn surfaces of steel balls. The curve demonstrates the relationship between the bearing length and height of the surface. In Figure 4.12d, the quasi-planar peaks coupled with

narrow grooves create the optimal geometry for bearing applications, as these features enable excellent load-bearing capabilities and lubricant retention.

8. Hybrid lubricated surface: optimal for tribological applications

Combination of benefits: The hybrid lubricated system, utilizing SiO_2-MoS_2 particles in castor oil, emerged as the most effective. Its quasi-planar peaks and narrow grooves provide ideal conditions for bearing applications. The smoother asperity profile and reduced roughness ensure lower friction and wear, while the negative skewness and platykurtic distribution enhance oil retention and load distribution.

The hybrid lubricated surface represents an excellent balance of surface roughness characteristics, making it ideal for applications requiring high load-bearing capacity and effective lubrication, such as in bearings. The combination of quasi-planar peaks, narrow grooves, and favourable roughness parameters ensures superior tribological performance.

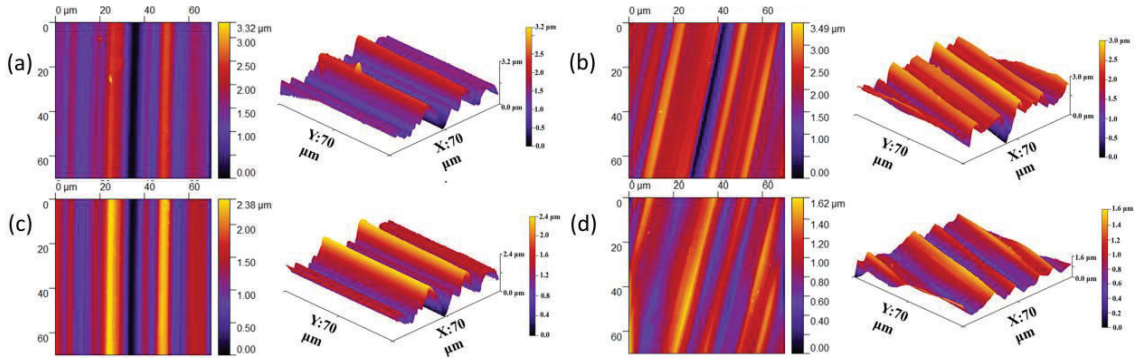

Figure 4.11: AFM based 2D and respective 3D images of worn steel balls from the tribotest carried at 392 N for 1 h at elevated temperature of 75 °C: (a) pure castor oil (CO) lubricated, (b) CO + 0.05% SiO_2, (c) CO + 0.05 wt% MoS_2, and (d) CO + 0.05 wt% SiO_2–MoS_2

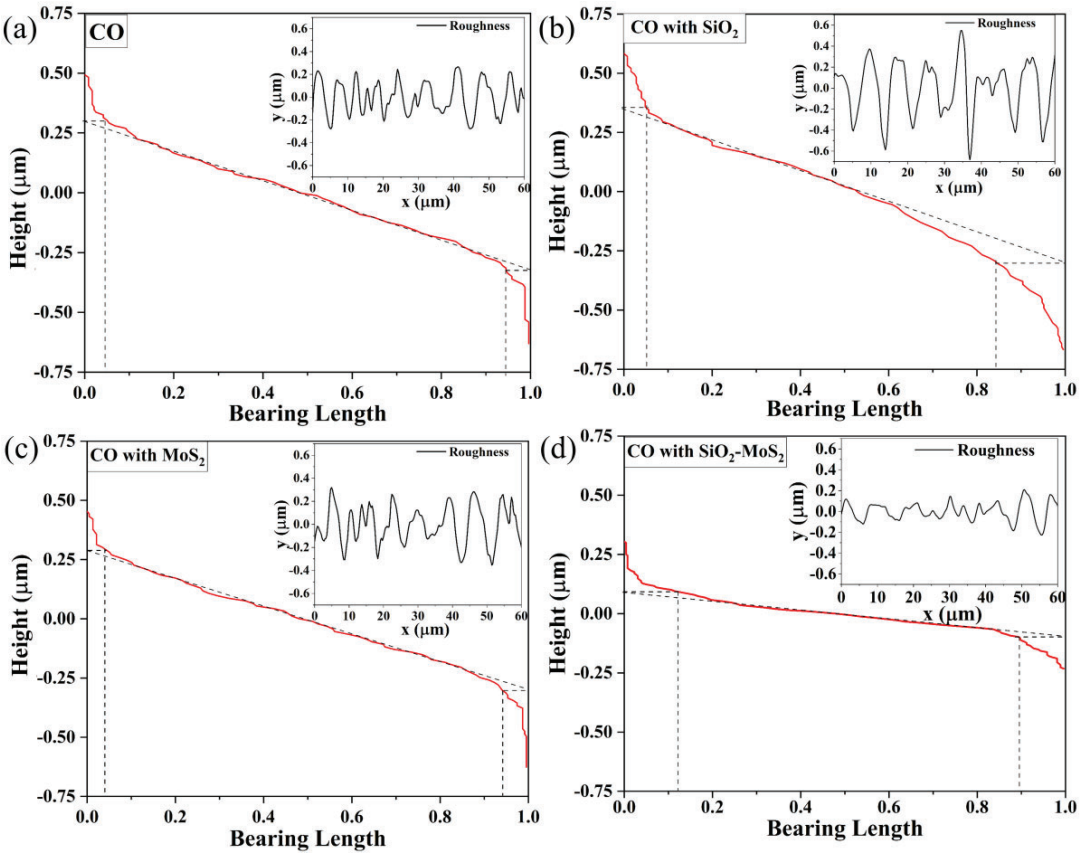

Figure 4.12: Bearing ratio curve drawn on height features versus bearing length fraction for all cases taken transverse to the scratch lay direction (test as per ASTM D-4172): (a) pure castor oil (CO) lubricated, (b) CO + 0.05% SiO_2, (c) CO + 0.05 wt% MoS_2, and (d) CO + 0.05 wt% SiO_2–MoS_2

4.4.3. XPS analysis of worn surface

Figure 4.13 depicts the XPS spectra for selected elements under various lubricated conditions. The Mo 3d spectra for hybrid and MoS_2 lubricated systems are shown in Figures 4.13a and 4.13b. The Mo (IV) peaks at 232.5 and 229 eV indicate the presence of MoS_2 on the surface. This confirms the formation of MoS_2-based tribolayers on both surfaces. Furthermore, the presence of a spectral feature at 235.6 eV implied the Mo $3d^{5/2}$ (VI) peak, corresponding to the formation of MoO_3 trioxide [98].

When comparing Figure 4.13a and 4.13b, the area ratio of the peak Mo (VI) is lower in the hybrid case. This indicates that the presence of silica in the hybrid system reduces the oxidation of MoS_2. Figure 4.13c and d show XPS spectra of SiO_2 for hybrid and pristine. There are no significant differences in the spectra, with the peak at 104.8 eV in both spectra corresponding to the Si 2p peak of SiO_2[99]. This confirms that silica is present in both hybrid and pristine, and that mending forms the deposition of their layer onto the tribo-surfaces in both cases.

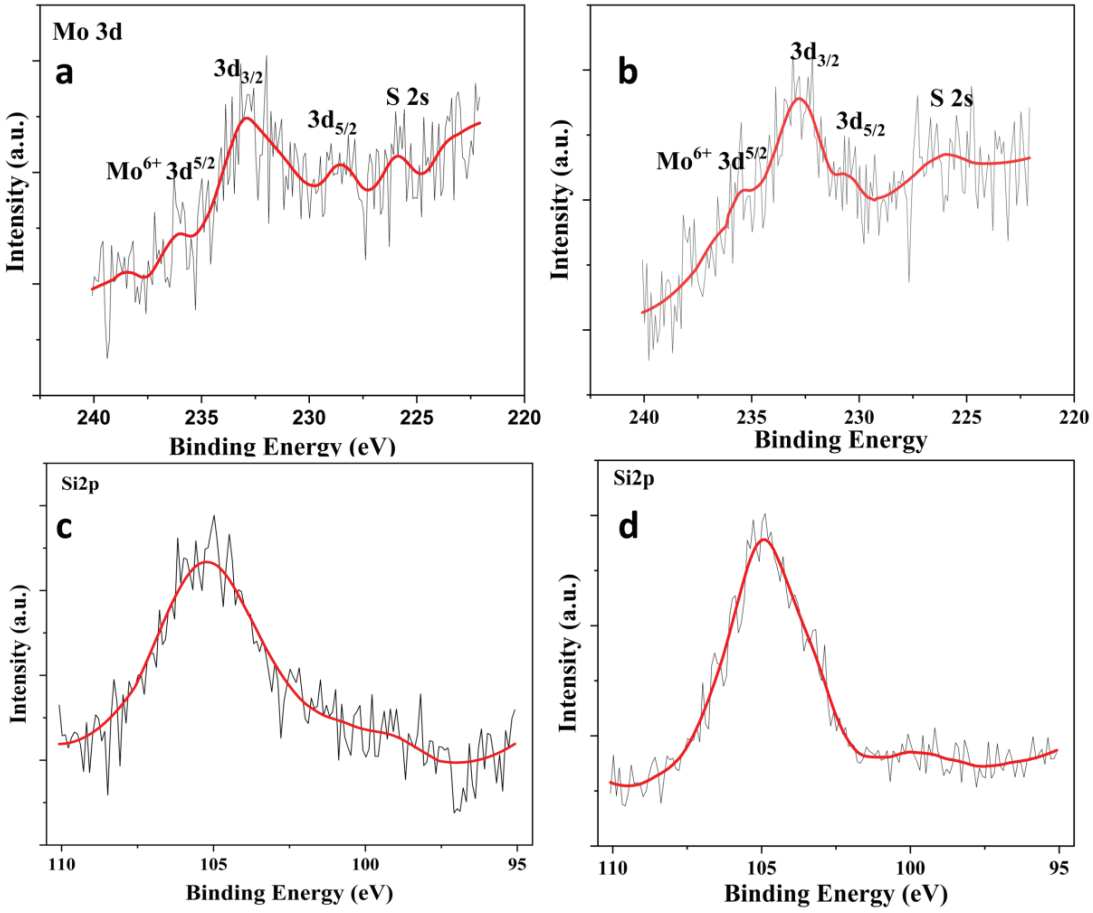

Figure 4.13: XPS Mo 3d spectra of worn surface taken from the tribotest (as per ASTM D-4172) with (a) *hybrid-lubricated and* (b) *pristine MoS_2-lubricated surface; Si2p spectra for wear surface of* (c) *hybrid lubricated and* (d) *pristine SiO_2 lubricated steel balls*

4.5. Wear debris analysis

4.5.1. XRD analysis of debris particles

Figure 4.14 shows the XRD results of wear debris. The XRD patterns show that the peak position of the MoS_2 lattice remains unchanged, indicating that the fundamental crystalline structure of MoS_2 is retained. However, the reduction in peak intensity suggests a loss of crystallinity or a decrease in the quantity of MoS_2 in the debris. This can occur due to:

- **Shearing or delamination**: During tribological testing, MoS_2, known for its layered structure, may undergo shearing, resulting in smaller crystallites or amorphous phases.
- **Oxidation or chemical reactions**: Some MoS_2 may oxidize or react with other components under the high temperatures and pressures of the tribological process.

Shift in silica peak

The silica peak shifting to the left by 2.36° is significant. According to **Bragg's Law**:

$$N\lambda = 2d\ sin\theta \qquad [4.1]$$

where:

- d is the interplanar spacing,
- θ is the Bragg diffraction angle.

A shift to a lower Bragg angle (θ) indicates an increase in the interplanar spacing (d). This increase in lattice parameter suggests the following possibilities:

- **Mechanical strain relaxation**: During the formation of the composite material, internal stresses might develop in the silica lattice. The wear process and subsequent breaking of composite spheres during tribo testing can relax these strains, resulting in an expansion of the lattice [100].

- **Amorphization or deformation**: The intense mechanical stresses during sliding or wear could introduce defects or disorder in the silica structure, affecting its crystallinity and shifting the diffraction peak.

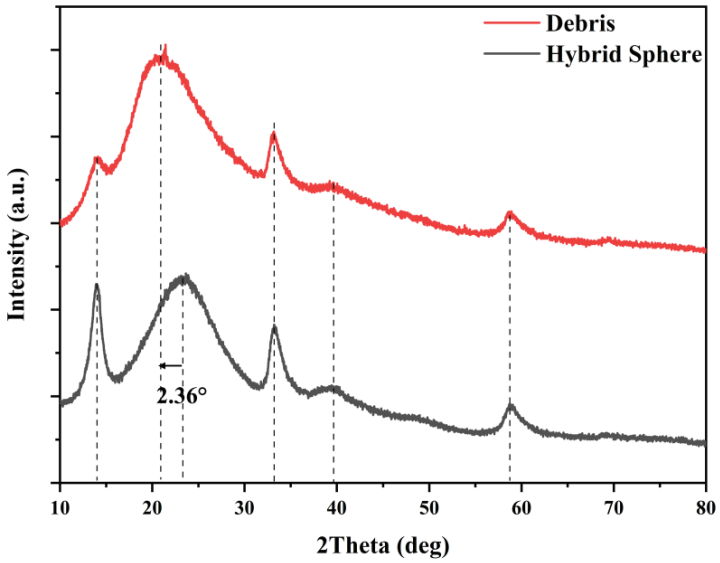

Figure 4.14 XRD patterns of wear debris

4.5.2. SEM analysis of wear debris

Figure 4.15 shows SEM images of wear debris separated from the tested oil of hybrid lubricated system. The features visible through the SEM are categorized into two structural groups. The first is a small particle between 30 and 50 nm in size, and the second is flattened broken fragments between 300 and 700 nm in size. The additives lost their spherical structure after the tribotest, indicating that the spheres may crack at the weakest point after flowing down into the interacting surface. The junction points of physically adsorbed silica to surface MoS_2 layers may be a possible crack initiation point due to the lower interaction force between the two sheets of MoS_2. Whereas Figure 4.16 shows EDS-based elemental mapping of wear debris, which depicts the presence of iron (Fe), and chromium (Cr) which are occurring in debris due to wear particles of steel ball.

The density of these elements from steel ball is quite low as compared to lubricant additives.

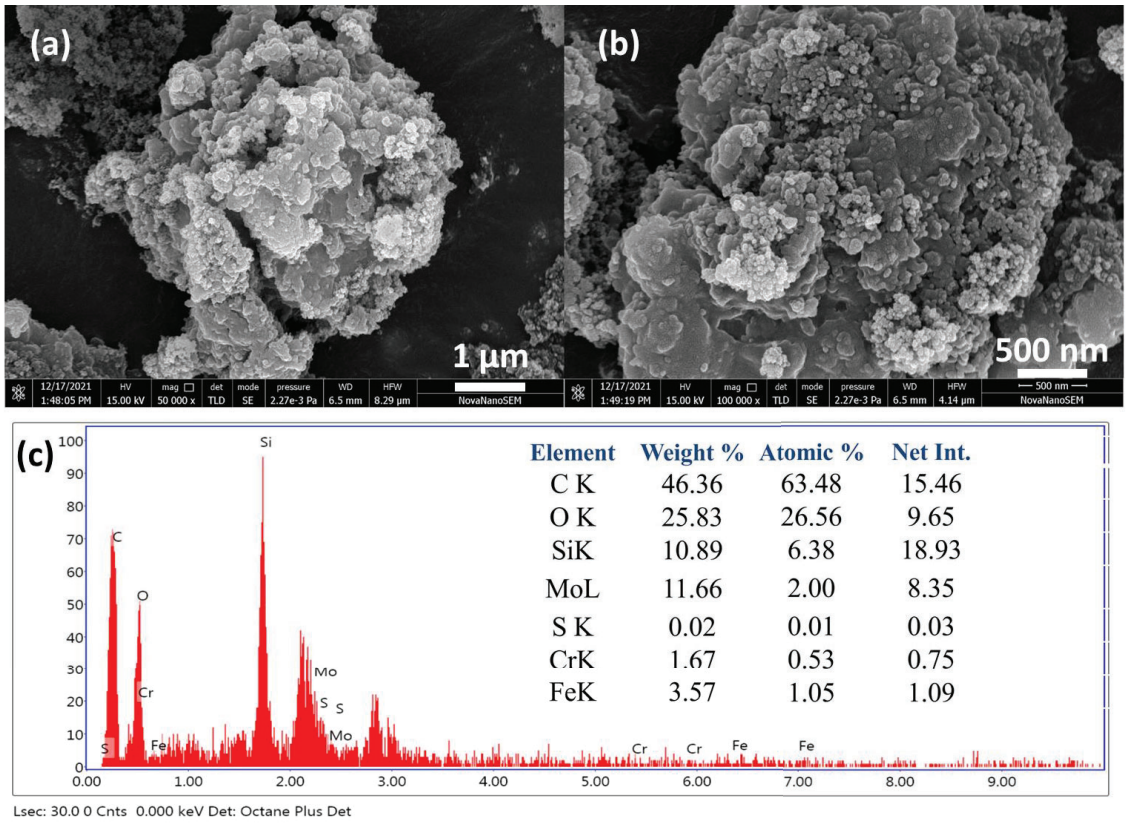

Figure 4.15 (a, b) SEM images of worn debris separated from the tested oil of hybrid lubricated system, (c) EDS spectra along with elemental analysis

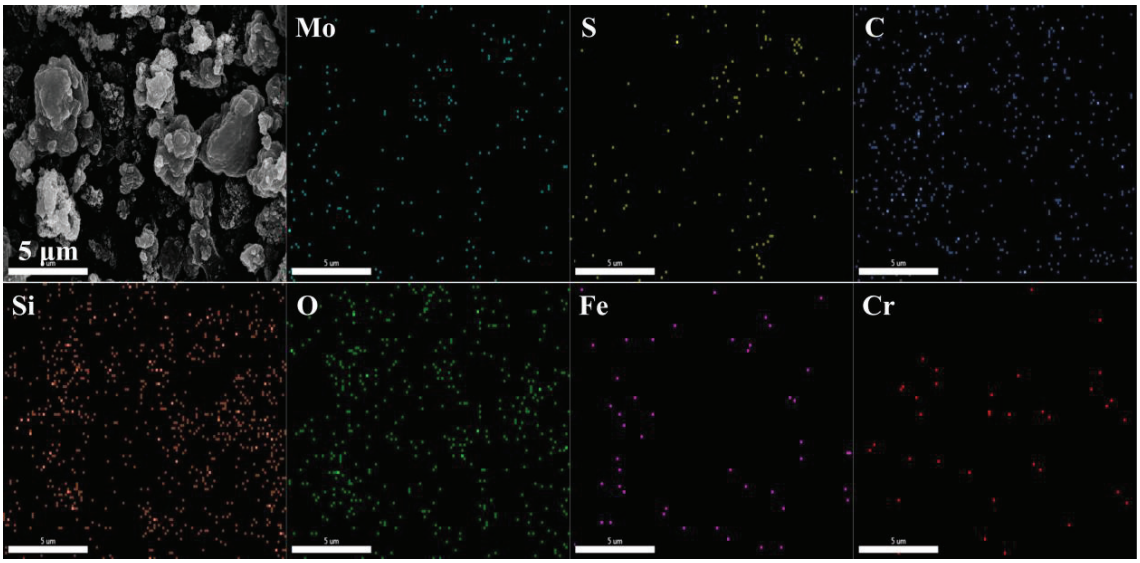

Figure 4.16: EDS elemental mapping of wear debris

Strain relaxation and composite behaviour

The composite spheres in the material are subjected to significant mechanical and thermal stresses during tribological testing. The strain initially present in these spheres may relax as the material fractures and debris forms. This process can be supported by the Scanning Electron Microscopy (SEM) images, which likely reveal

- **Fractured composite spheres**: Indicating that the strain accumulated during the formation of the spheres is released during tribo-testing.
- **Wear debris morphology**: Highlighting that the debris consists of smaller particles or fragments, suggesting brittle fracture or delamination processes.

Implications for tribological performance

- The retention of the MoS_2 lattice structure, albeit with reduced intensity, suggests that MoS_2 continues to play its role as a solid lubricant, reducing friction and wear.

- The shift in silica peak and the observed strain relaxation point to the composite's ability to adapt under mechanical stress. This may indicate a balance between brittleness and ductility, influencing wear mechanisms and debris formation.
- These findings underscore the importance of optimizing composite sphere formation and testing conditions to improve wear resistance and overall tribological performance.

By correlating XRD data with SEM observations, a comprehensive understanding of the wear mechanisms can be achieved, aiding in the design of more robust materials for tribological applications.

4.6. Lubrication mechanism

Sphere entry and initial contact

- When the hybrid sphere comes into contact with the tribological interface, it begins by rolling or sliding under the applied load, acting as a load-bearing element.
- XRD Analysis: Figure 4.14 shows that silica particles within the hybrid sphere start breaking into smaller fragments under stress. The shift of silica's diffraction peak to the lower 2θ confirms this phenomenon, indicating an increase in lattice spacing as the material fractures.
- The rolling action of the sphere dominates at this stage, facilitating uniform load distribution.

Sphere breakage and wear mechanism

- Silica-Abrasive Interaction: Figure 4.9 highlights that silica plays a dominant role in abrasive wear, leaving etched wear marks on the surface. In the hybrid case, similar dashed marks appear, indicating localized interactions where silica particles etch the surface alongside the MoS_2.

- As silica breaks into smaller fragments, these particles can:
    - Engage in abrasive wear, modifying surface topography.
    - Fill smaller grooves, contributing to the mending effect.
- Tribolayer Formation: The elemental map in Figure 4.10 reveals the formation of a tribolayer on the surface, composed of silica fragments and MoS_2 sheets. This tribolayer acts as a protective interface, reducing direct contact and wear.

Lubrication by mending effect

- **Silica role**: Due to its smaller size after breaking, silica particles can fill finer surface grooves. This action contributes to the mending effect, smoothing out surface valleys and reducing surface roughness.
- **MoS_2 role**: MoS_2 sheets, known for their layered structure, can slide easily and cover larger grooves. This leads to a reduction in friction and the formation of a lubricating film.
- The synergistic interaction of these two mechanisms results in a polished, smooth surface, as confirmed by the AFM data in Figure 4.11, which shows reduced roughness and valley depth.

Surface adaptation and skewness

- The presence of silica increases surface skewness, which enhances its ability to hold lubricant. This adaptation ensures the surface is optimized for lubrication retention, contributing to the overall tribological performance.

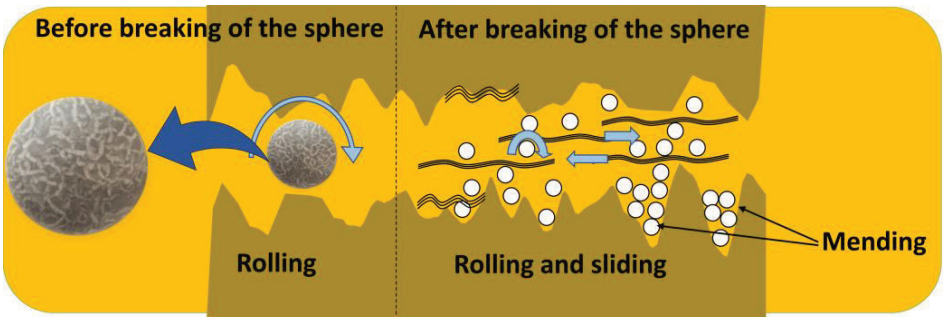

Figure 4.17: Lubrication mechanism of SiO_2-MoS_2 hybrid lubricant

Mechanism summary

- A schematic representation of the lubrication mechanism for the hybrid sphere is shown in Figure 4.17. The mechanism consists of three stages:
    1. **Rolling the sphere**: The hybrid sphere initially rolls over the surface, spreading load and reducing friction.
    2. **Release of entrapped particles**: Under stress, the sphere breaks, releasing silica fragments and MoS_2 sheets into the interface.
    3. **Rolling and sliding combination**: A combination of rolling and sliding action occurs, where silica fills smaller grooves, and MoS_2 sheets form a lubricating layer over larger grooves.

4.7. Chapter summary

A novel method for synthesizing spherical SiO_2-MoS_2 particles was developed and characterized using XRD and EDS analyses, with SEM confirming their spherical morphology. The lightweight particles were produced through the rapid drying of a gelled structure. Tribological studies demonstrated that a 0.05 wt% hybrid lubricant reduced the coefficient of friction (COF) by 46% and wear volume by 58% compared to pure oil. The hybrid lubricant outperformed systems with SiO_2 or MoS_2 alone due to the synergistic interaction between the two components.

While wear mechanisms for pure oil and MoS_2 systems were dominated by adhesive wear and SiO_2 systems by abrasion, the hybrid system exhibited a combination of adhesive and abrasive wear. Post-test wear debris analysis revealed the presence of all hybrid elements and surface metals, indicating particle fragmentation during lubrication. The hybrid spheres broke upon entering the tribo-surfaces, forming a stable tribolayer of exfoliated MoS_2 combined with silica fragments. This layer, along with the combined rolling and sliding mechanism, contributed to the reduction in friction and wear.